Deposition of diamond films on single crystalline silicon carbide substrates
Peer-reviewed author version

Deposition of diamond films on single crystalline silicon carbide substrates

Debarati Mukherjee[1,2], Filipe Oliveira[3], Simone Camargo Trippe[4], Shlomo Rotter[7], Miguel Neto[3], Rui Silva[3], Awadesh Kumar Mallik[5], Ken Haenen[5], Carl-Mikael Zetterling[6], Joana Catarina Mendes[1,8*]

[1]*Instituto de Telecomunicações, Campus Universitário de Santiago, 3810-193 Aveiro, Portugal*

[2]*Department of Electronics, Telecommunications and Informatics, University of Aveiro, 3810-193 Aveiro, Portugal*

[3]*CICECO, Department of Materials and Ceramic Engineering, University of Aveiro, 3810-193 Aveiro, Portugal*

[4]*Centro Universitário FEI, Physics Department, São Bernardo do Campo, SP, Brazil*

[5]*Institute for Materials Research (IMO), Hasselt University, and IMOMEC, IMEC vzw, Wetenschapspark 1, 3590 Diepenbeek, Belgium*

[6]*KTH Royal Institute of Technology, Dept. of Electronics and Embedded Systems, Kista, Sweden*

[7]*Smart Diamond Technologies Lda, Aveiro, Portugal*

[8]*Centre for Mechanical Technology and Automation, University of Aveiro, 3810-193 Aveiro, Portugal*

[*] *joanacatarina.mendes@av.it.pt*

Abstract

Silicon carbide (SiC) is a wide band gap material that is slowly but steadily asserting itself as a reliable alternative to silicon (Si) for high temperature electronics applications, in particular for the electrical vehicles industry. The passivation of SiC devices with diamond films is expected to decrease leakage currents and avoid premature breakdown of the devices, leading to more efficient devices. However, for an efficient passivation the interface between both materials needs to be virtually void free and high quality diamond films are required from the first stages of growth. In order to evaluate the impact of the deposition and seeding parameters in the properties of the deposits, diamond films were deposited on SiC substrates by hot filament chemical vapor deposition (HFCVD). Before the seeding step the substrates were exposed to diamond growth conditions (pre-treatment PT) and seeding was performed with a solution of detonation nanodiamond (DND) particles and with 6-12 and 40-60 μm grit. Diamond films were then grown at different temperatures and with different methane concentrations and the deposits were observed in a scanning electron microscope (SEM); their quality was assessed with Raman spectroscopy.

Keywords

DND seeding; CVD diamond; device passivation; SiC

Research Highlights

Diamond films were deposited on SiC substrates; the pre-treatment of the substrate together with low deposition temperatures induce the lateral growth of the diamond crystals during the initial stages of diamond deposition.

Films obtained after seeding with 6-12 μm grit show higher quality when compared to films obtained after seeding with DND particles. These results are attributed to the existence of an sp^2 shell surrounding the DND core particles.

1. Introduction

Silicon carbide (SiC) is a wide band gap material that can be used in applications where silicon (Si) components reached the performance limits. When the first SiC power device came to the market, back in 2001, expectations regarding its widespread use for high-efficiency power electronics were very high [1]. 6'' SiC wafers are still much more expensive than their Si counterparts, however SiC intrinsic properties (lower on-resistance and high temperature operation capability) translate into higher efficiency, smaller volume and lower system costs. For high temperature operation, such as in the electric vehicles industry, SiC components are often the only realistic technical solution. At the present moment, SiC devices such as bipolar integrated circuits operating at 500°C have already been reported [2]. However, as reverse voltage levels increase, the higher electric fields at the surface may lead to premature breakdown or excessive leakage currents, raising the need to passivate the devices surface with adequate materials.

Diamond films deposited by chemical vapor deposition (CVD) have a large reverse breakdown field and high thermal conductivity, and can be used to passivate SiC devices. Depositing diamond on foreign substrates requires the previous enrichment of their surface with diamond nano-particles; failure to do so results in the growth of 10^2-10^3 cm^{-2} isolated diamond crystals that do not form a closed film [3]. The simplest method is to scratch or abrade the substrate with diamond or an abrasive grit [4]. Ultrasonic (US) seeding [3] can be used to seed complex shapes and the possibility of choosing grit size allows a finer control of the nucleation process. US seeding with a colloidal solution of detonation nanodiamond (DND) enables nucleation densities in excess of 10^{12} cm^2 [5–9]. DND suspensions with different ζ potential can be obtained with proper functionalization of the particles' surface [10]; in particular, suspensions with positive ζ potential have been used to grow diamond films on gallium nitride (GaN) substrates [11] and Au (gold) films [12]. Bias-enhanced nucleation (BEN) [13,14] employs *in-situ* surface bombardment in the gas phase by carbon species through the application of negative bias on the substrate. This seeding technique has been used to grow highly-oriented diamond films on multilayered iridium (Ir) substrates like Ir/yttria-stabilized zirconia/Si [15] or Ir/SrTiO3/Si [16] and to fabricate devices like mechanical microactuators [17], field effect transistors [18] and high-performance Schottky diodes [19]. Other seeding methods include dipping the substrate in a suspension containing diamond nanopowders [20,21], ink jet printing [22–24] or electrostatic self-assembly [25,26].

High seeding or nucleation densities are usually regarded as promoters for the growth of closed thin diamond films. A high nucleation density indeed facilitates the growth of diamond on non-diamond substrates [27–29], however this may not be the only important factor when diamond films are to be used as passivation or heat dissipation layers. As the seeded substrate is introduced in the CVD system, the seed centers grow three dimensionally until they coalesce with each other (the so-called incubation period), thus kinetically restricting the supply of gas radicals approaching the substrate. This creates a void and the gas radicals trapped in these crevices can coalesce in a non-diamond phase (graphitic or amorphous carbon) [8]. These voids (as the ones reported in [8,9,25]) have an obvious detrimental effect in the passivation of electric defects or in the extraction of heat from the substrate. In addition, the boundaries between individual diamond nuclei are saturated with non-sp^3 bonds, meaning that a very large nucleation density implies a high percentage of non-diamond bonds. Again this is detrimental for electric passivation or heat extraction. On one side, if the density of grain boundaries is high enough, the latter may provide channels through which the charge carriers can flow [30]; on the other side, the grain boundaries induce phonon scattering and also compromise the thermal conductivity of the diamond film [31,32].

The density of voids and grain boundaries at the nucleation surface can be diminished by enhancing the lateral growth of the grains during the initial stages of diamond deposition. This can be achieved by exposing the substrate surface to typical diamond growth conditions for a short period of time, prior to the seeding step (the pre-treatment (PT) described in [33,34]). This procedure (commonly referred to as NNP) enriches the surface with a nm-thick carbon layer that improves the dispersion of the diamond particles during the seeding procedure [34] and induces a lateral growth mode during the early stages of diamond formation, which in turn accelerates grain coalescence and diminishes the number of voids [33]. This was experimentally verified by Sumant *et al.* [35], who studied thoroughly the nucleation surface of nanocrystalline diamond (NCD) films deposited on Si substrates pre-treated and seeded with diamond nanopowders; the roughness of the nucleation surface was as low as 0.3 nm and the sp^2 content was only 1.8%, in comparison with 0.7% on the top side.

To obtain an interface with a defect density as low as possible, the previous optimization of the CVD parameters should be performed. Substrate temperature and CH_4/H_2 ratio directly influence the morphology and growth rate of the diamond film. CVD diamond growth typically requires substrate temperatures between 500 and 1200°C; as substrate temperatures drift above or below from this interval, the film shifts to graphite or diamond-like-carbon (DLC) deposits, respectively. The growth rate reaches a maximum around 1000°C and the substrate temperature influences significantly the film morphology [36]. Due to the difference in the thermal expansion coefficients (TEC) of diamond and substrate, the deposition temperature impacts directly the thermal stress at the interface. When comparing the TECs of diamond, Si and SiC (1.0 [37], 2.6 [38] and 3.08 ×10^{-6} K^{-1} [39], respectively) it can be concluded that the mismatch effect is more critical in SiC than in Si. The size and type of the diamond particles used for the US seeding may also influence the nucleation density and consequently the quality of the interface and the uniformity of the diamond coating, so this parameter should also be optimized.

This paper reports low temperature deposition of diamond films by hot filament CVD (HFCVD) on epitaxial and polished SiC samples using NNP. The parameters that were varied include seeding suspension, deposition temperature and CH_4/H_2 ratio. The deposited films were observed by scanning electron microscopy (SEM) and the quality was accessed with Raman spectroscopy.

2. Materials and methods

A total of fourteen 10×10 mm^2 double side polished 300 μm-thick 4H-SiC samples were used in this work. Additional films were deposited on 4 n-type epitaxial 6H-SiC wafers. The roughness of both polished and epitaxial samples was lower than 0.3 nm. The depositions were performed in a home-made HFCVD system with rhenium (Re) filaments at 50 mbar. The temperature was measured by a thermocouple touching the back of a sacrificial SiC substrate.

The SiC substrates were ultrasonically cleaned using acetone followed by ethanol and were air-blown dried before being inserted in the HFCVD system for the PT step [33]. The surface of the SiC substrates from series A was partially covered with flat Si samples during this step; in the remaining experiments (series B, C & D) the whole surface of the SiC was exposed to the gas phase. Seeding was performed after the PT step for 90 minutes using one of three different types of diamond suspension: (i) 200 mg of 40-60 μm diamond grit dispersed in 20 ml ethanol, (ii) 200 mg of 6-12 μm diamond grit dispersed in 20 ml ethanol and (iii) 10 nm clusters of 4-5 nm detonation nanodiamond (DND) particles dispersed in dimethyl sulfoxide (DMSO) (with a ζ potential of (35 ± 5) mV) diluted in ethanol (1:3 ratio).

The diamond grits and the DMSO DND suspension were supplied by Saint-Gobain Ceramic Materials and International Technology Center, respectively. After being seeded the SiC samples were again introduced in the system for diamond deposition. The PT, seeding and deposition conditions for all the samples are listed in Table 1; for convenience the sample name reflects the processing history of each sample, that is, sample names with same partial name mean that that particular procedure was performed to all samples simultaneously.

After diamond deposition the samples were observed in a Hitachi SU70 SEM. Micro Raman measurements were performed at room temperature with a WITEC Confocal Raman Microscope Alpha300 R. The spectra were excited with a 532 nm laser and with a maximum power of 45 mW.

Series	Sample name[1]	Substrate[2]	Pre-treatment (PT)			Seeding (S)	Growth (G)			Grain size (nm)	Nucleation density (cm^{-2})	FWHM (cm^{-1})
			CH$_4$/H$_2$ (%)	Temp. (°C)	Duration (min)		CH$_4$/H$_2$ (%)	Temp. (°C)	Duration (min)			
A[3]	POL_PT1_S1_G11	Pol	1	600	60	40-60 μm	1	500	120	500-600	N.A.	
	POL_PT1_S1_G12						1	600	60	250-350	N.A.	
	POL_PT1_S1_G13						1.5	500	90	400-600	N.A.	
	POL_PT1_S1_G14						1.5	600	30	200-300	N.A.	
B	POL_PT2_S2_G21	Pol	1	600	60	40-60 μm	1	500	120	600-800	4×10^8	
	POL_PT2_S2_G22						1	600	60	200-300	6×10^8	
	POL_PT2_S2_G23						1.5	500	90	400-600	4×10^8	
	POL_PT2_S2_G24						1.5	600	30	150-250	5×10^8	
C	POL_PT2_S3	Pol	1	600	60	4-5 nm	--	--	--	--	9×10^6 [4]	--
	POL_PT2_S3_G3						1	500	60	50-100	N.A.	63
	POL_PT2_S3_G4						1	500	180	333-550	N.A.	19
	EPI_PT3_S4	Epi	1	600	60	6-12 μm	--	--	--	--	4×10^6 [4]	--
	EPI_PT3_S4_G3						1	500	60	150-350	N.A.	20
	EPI_PT3_S4_G4						1	500	180	350-750	N.A.	16
D	EPI_PT4_S5_G5	Epi	1	500	60	6-12 μm	1	500	60	125-225	N.A.	19

Table 1. Deposition conditions.

[1] The sample name reflects the processing history of each sample

[2] Epi – epitaxial SiC; Pol – polished SiC

[3] The substrate was partially covered with a Si piece during the PT step

[4] Spontaneous nucleation density

3. Results and discussion

The samples from series A were given 1 hour PT with 1% CH$_4$/H$_2$ at 600°C. Following the PT step, the Si piece was removed, seeding was performed with large 40-60 μm diamond grit and diamond was deposited according to the conditions in Table 1. Figures 1a and b show low magnification SEM images of samples POL_PT1_S1_G11 and POL_PT1_S1_G14. The diamond deposits are extremely non-uniform and the shade of the Si piece (marked with a red line) is clearly visible in the SEM images. Figures 1c and d show higher magnification images of the regions marked with green arrows in Figures 1a and b. The films deposited on samples POL_PT1_S1_G12 and POL_PT1_S1_G13 follow the same trends and are not shown. The SEM images show that the diamond films have fully coalesced close to the vicinity of the Si pieces. On the contrary, only isolated diamond crystals were deposited in the remaining regions. Since both seeding and growth cycles were performed with the surface of the SiC substrates fully exposed, the variation of the diamond films characteristics reflects a variation of the local carbon supply during the PT step. This may be explained in case the gases infiltrated below the Si pieces, trapping the carbon radicals in the vicinity of the Si piece and artificially increasing the local carbon supply during the PT step. It is known that the thickness of the PT film increases with the CH$_4$/H$_2$ ratio [33], so the trapping of carbon

radicals would translate in an increased PT film thickness near the vicinity of the Si piece. During the growth cycle, the existence of regions with an augmented carbon supply would in turn result in the deposition of a denser film.

The denser zones (marked with red arrows) were observed under higher magnification, revealing films with different trends. The deposition times are different for all the samples and it can be seen that for the same temperature (Figures 1e and g, Figures 1f and h) longer deposition times resulted in larger crystals, as expected (Table 1). The grains of films deposited at 600 °C (Figures 1f and h) are more faceted than the ones deposited at 500°C. This influence of the substrate temperature on the film morphology has been widely reported in the literature [40]. A closer analysis to the surface of the diamond films further suggests that the crystals obtained with lower deposition temperatures and CH_4/H_2 rates are larger and flatter. These deposition conditions translate in lower growth rates; however, at the same time, the PT film acts as a steady carbon supply during the first moments of deposition. This extra carbon source, combined with the lower growth rates induced by the substrate temperature and gas composition, result in the lateral growth mode of the crystals during the initial moments of deposition. Figure 2a shows the Raman spectra obtained from the denser zones. The Raman spectrum obtained from the SiC substrate alone is included as a reference. The diamond peak is centered around 1332 cm^{-1} and is considerably broad for all films, with the exception of the film deposited at 500°C with 1.5% CH_4/H_2. However, as discussed above, if the gas molecules were trapped below the Si surface the local carbon content changed, so it is not possible to relate the quality of the films with the deposition conditions. A weak band centered around 1150 cm^{-1} is seen in all the films, indicating the presence of NCD or trans-polyacetylene. The films deposited with 1% CH_4/H_2 show the G-band at 1590 cm^{-1}. An additional broad band centered at $\cong$1500 cm^{-1} is seen in some spectra, however the strong SiC band centered at 1520 cm^{-1} makes it difficult to distinguish the signals coming from substrate and film.
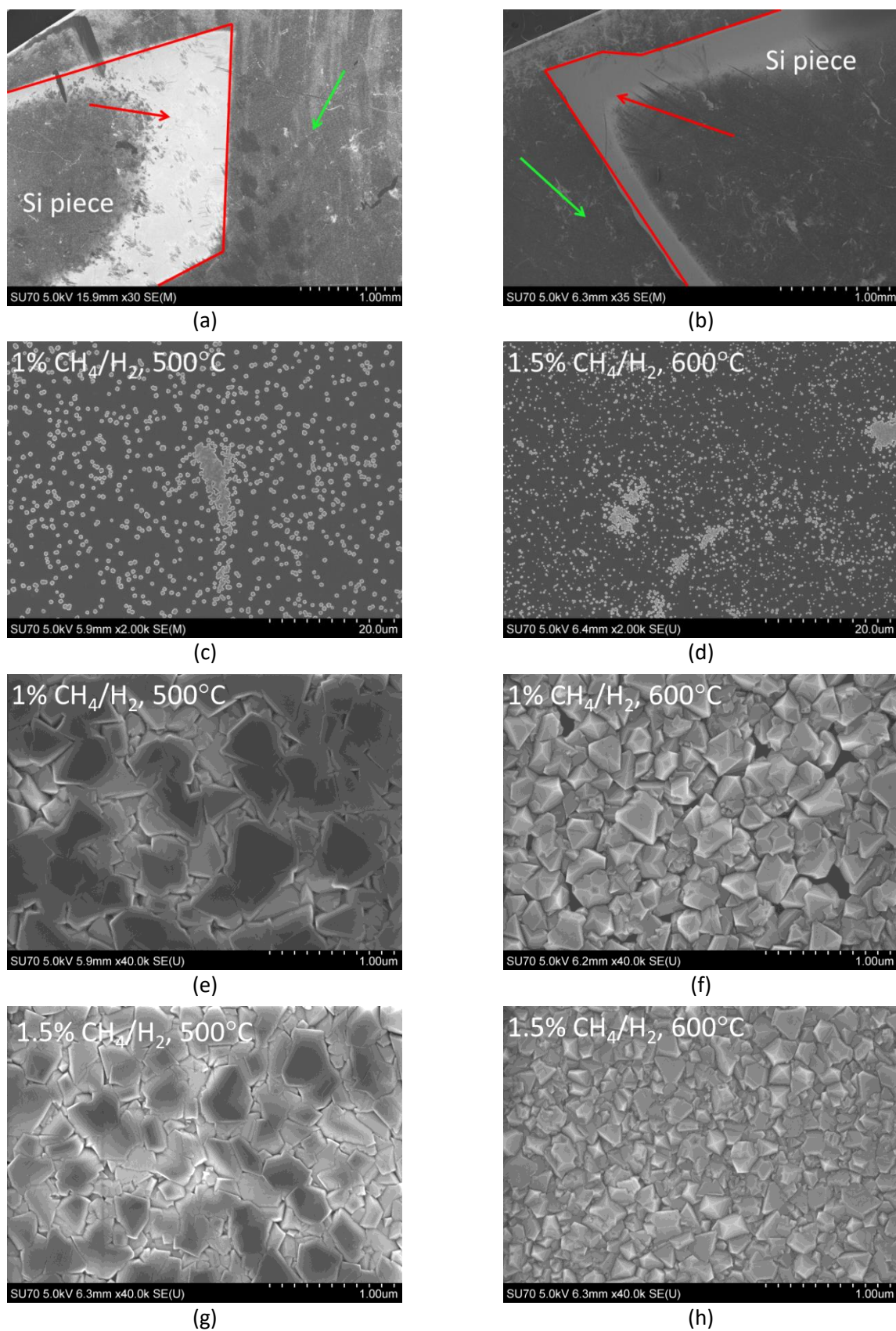
Figure 1. Low magnification SEM images of series A samples (a) POL_PT1_S1_G11 and (b) POL_PT1_S1_G14. Magnified images of areas marked with green arrows, samples (c) POL_PT1_S1_G11 and (d) POL_PT1_S1_G14. SEM images of denser zones marked with red arrows, samples (e) POL_PT1_S1_G11, (f) POL_PT1_S1_G12, (g) POL_PT1_S1_G13 and (h) POL_PT1_S1_G14.
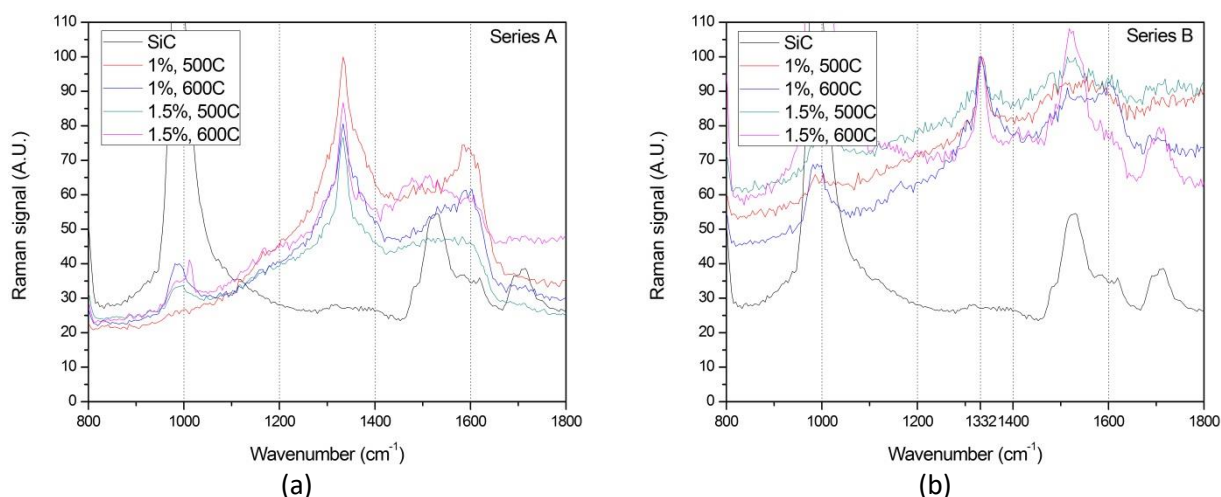
Figure 2. Raman spectra of samples from series (a) A and (b) B.

The following set of samples (series B) was prepared under the same conditions as series A (Table 1), but the PT was performed on the whole surface of the SiC samples. The deposited films are uniform all over the sample but they did not coalesce to form closed films (Figure 3). The films coalescence decreases from samples 3a to 3c, 3b to 3d; in other words, 1% CH_4/H_2 and 500°C is the condition which favored the effective closing of the films (thanks to the lateral growth of the grains), whereas 1.5% CH_4/H_2 and 600°C did not promote the formation of closed films. This somewhat counter intuitive fact (it is the general understanding that higher substrate temperatures and CH_4/H_2 concentration promote diamond growth, irrespective of the film quality) again suggests that the carbon in the PT film plays a crucial role in the early growth of the diamond crystals. It is interesting to note that the shape of the individual crystals follows the trend observed in series A, since crystals deposited at 500 °C (Figures 3a and c) have a tendency to be larger and flatter. The average size of the crystals in samples from series A and B deposited under the same conditions is also similar (Table 1). The nucleation density in the four samples is listed in Table 1 and is in the range 6×10^8 cm^{-2}; the differences are ascribed to the difficulty in identifying all the individual crystals in samples POL_PT2_S2_G21 and POL_PT2_S2_G23. From these results it can be concluded that the seeding of the SiC substrates with the 40-60 μm diamond is not effective.
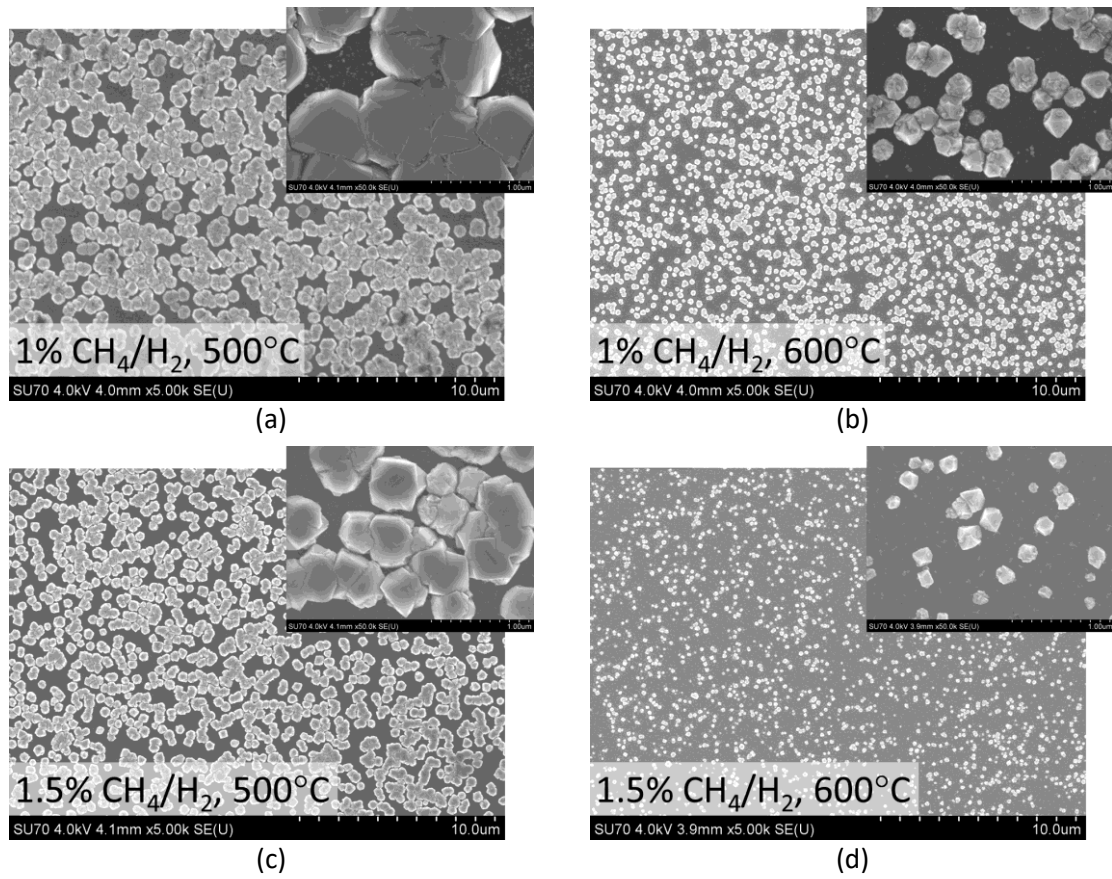
Figure 3. SEM images of series B samples (a) POL_PT2_S2_G21, (b) POL_PT2_S2_G22, (c) POL_PT2_S2_G23 and (d) POL_PT2_S2_G24. Insets: details of isolated grains.

Following these results with large 40-60 μm grit, the subsequent seeding cycles were performed with 4 nm DND and 6-12 μm grit. The four samples from series C (two epitaxial and two polished) were initially given a similar PT step (1 hour at 600°C and 1% CH_4/H_2 ratio). After the PT, the polished samples were seeded with 4 nm DND suspension and the epitaxial samples were seeded with 6-12 μm diamond grit. Figures 4a and c show low magnification images of the surface of the seeded SiC samples. Both samples show isolated crystallites that grew spontaneously on the SiC surface during the PT step, with a density of 9 and 4 ×10^6 cm^{-2} for DND and 6-12 μm grit, respectively. The surface of the polished sample shows approximately twice more crystals; even though the difference is not considerable, this may indicate that the polishing of the SiC wafer increases the number of nucleating sites for diamond growth. The inset in Figure 4a is a magnification of the top-right area of the image where polishing lines resulting from the polishing of the SiC wafer are clearly seen. It is interesting to note that these lines were not visible before the PT and seeding procedures. The polishing of hard materials like SiC of WC-Co is routinely performed with diamond grit, starting with large particles and then refining the particle size until the final desired roughness is met. However, even though the final roughness may be very low (<0.3 nm), the final polishing may not remove the deeper defect lines caused by the initial polishing with large diamond grit– and that offer improved sites for diamond nucleation. These polishing lines can also be seen in the nucleation surface of diamond films grown on polished Si substrates [9]. However, and despite these lines, it should be noted that the roughness of both substrates is similar and, as a consequence, the particular type of substrate is not expected to have any major influence on the morphology and quality of the diamond films. Instead, any meaningful differences are attributed to the influence of the particular suspension (DND vs. 6-12 μm grit) used to seed the substrates. Going back to

Figures 4b and d, from these images it can be concluded that seeding with both diamond suspensions results in a uniform surface coverage. However, when the seeding is performed with DND suspension the nanoparticles tend to form agglomerates that can be as large as 70 nm on the surface (Figure 4b). Even though the size of the individual DND particles in the suspension is 4-5 nm, it is known that they tend to form primary aggregates with average sizes below 30 nm that are very difficult to separate by simple sonication. These aggregates have a tendency to further agglomerate due to the inherent tendency to reduce the surface energy [41]. The presence of both primary and secondary aggregates is clearly seen on the surface of the sample seeded with DND suspension. Seeding with 6-12 μm grit gives different results. When the 6-12 μm diamond particles hit the SiC substrate during the US seeding, small diamond particles are chipped off from the larger particles, resulting in a uniform "seeding mat". Some 40-70 nm-sized clusters composed of diamond particles are also present on the SiC surface (Figure 4d). A large crystal that grew during the PT step can be seen in the top-left corner of sample seeded with DND (Figure 4b).
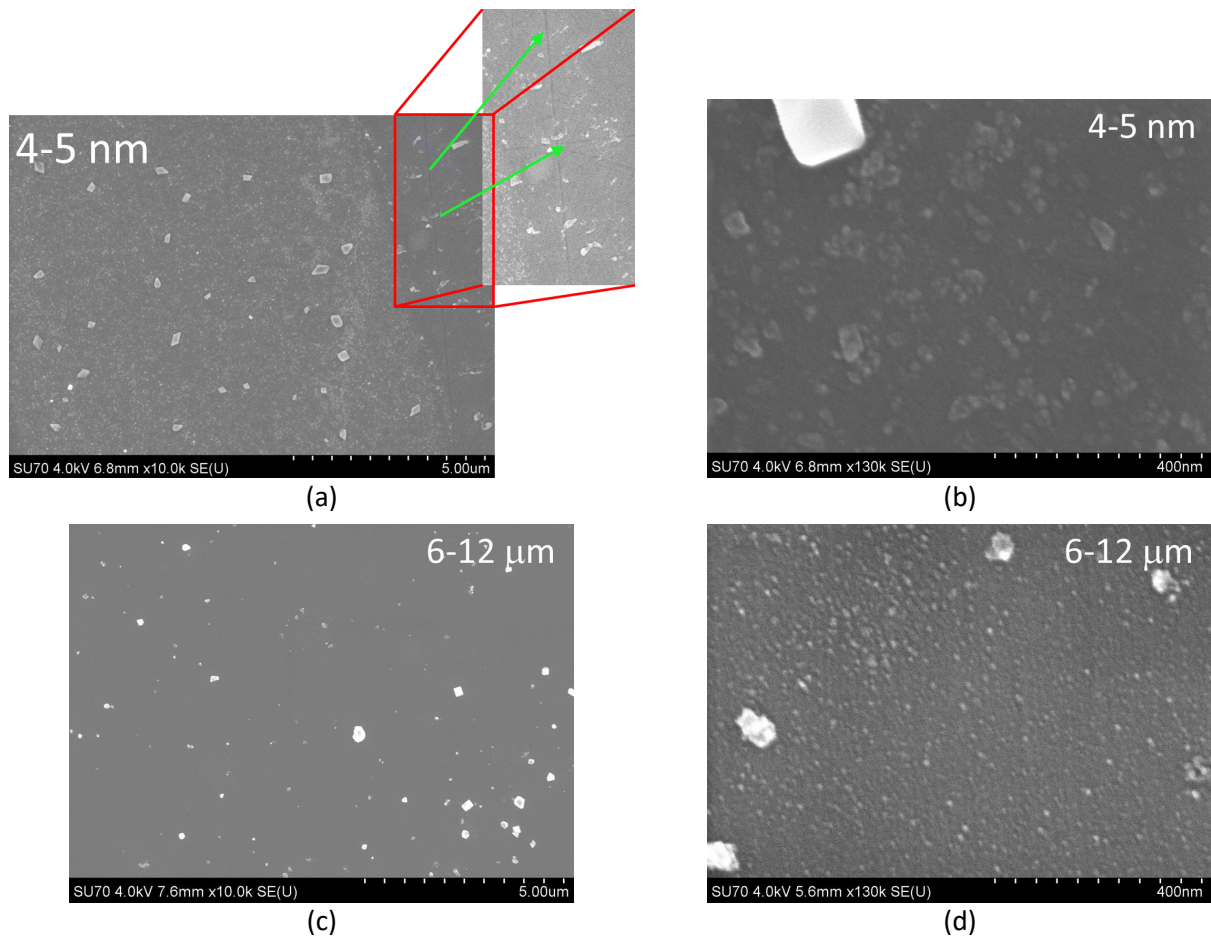

Figure 4. SEM images of series C samples after PT and seeding cycles; (a), (b) POL_PT2_S3; (a) inset: visible polishing lines; (c), (d) EPI_PT3_S4.

The pre-treated and seeded series C samples were again introduced in the system. Diamond was deposited for one and three hours using the conditions that led to the largest crystals (500 °C and 1% CH_4/H_2 ratio) and a polished and an epitaxial (seeded with DND and 6-12 μm diamond particles, respectively) SiC sample were coated in each run. The morphology of the deposited films can be seen in Figure 5. After only one hour of growth at 500 °C, the sample seeded with DND suspension shows a completely closed and uniform film (Figure 5a). On the other hand, the film deposited on the sample

seeded with 6-12 μm diamond grit looks very uniform, despite the presence of some small gaps (marked with a red rectangle in Figure 5b). The inset shows a magnified view of a ≈400 nm hole. Curiously, the crystals on sample seeded with 6-12 μm are larger than the crystals on sample seeded with DND particles (150-350 nm against 50-100 nm after one hour diamond growth). In the case of the grit-seeded sample, the surface was covered with a complete layer of diamond nanoparticles that chipped off from the larger diamond particles during the US seeding (Figure 4d). Once under growth conditions, these particles start growing immediately, without any incubation period. On the other hand, it is known that commercial DND particles typically have an outer shell of graphitic or amorphous carbon [42,43]. This shell delays the effective growth of the diamond seeds– thus explaining the difference in the size of the grains on samples seeded with grit and DND after one hour of growth. Despite the fact that the film obtained with DND seeding has smaller crystals, it is fully closed and no holes can be seen, suggesting that seeding with DND particles results in a higher nucleation density than seeding with 6-12 μm grit. After three hours growth, both films are closed and uniform (Figure 5c, d). The grains of sample EPI_PT3_S4_G4 are again slightly larger than the grains of sample POL_PT2_S3_G4 (350-750 nm against 300-550 nm), even though the difference is not as marked as after one hour of growth.
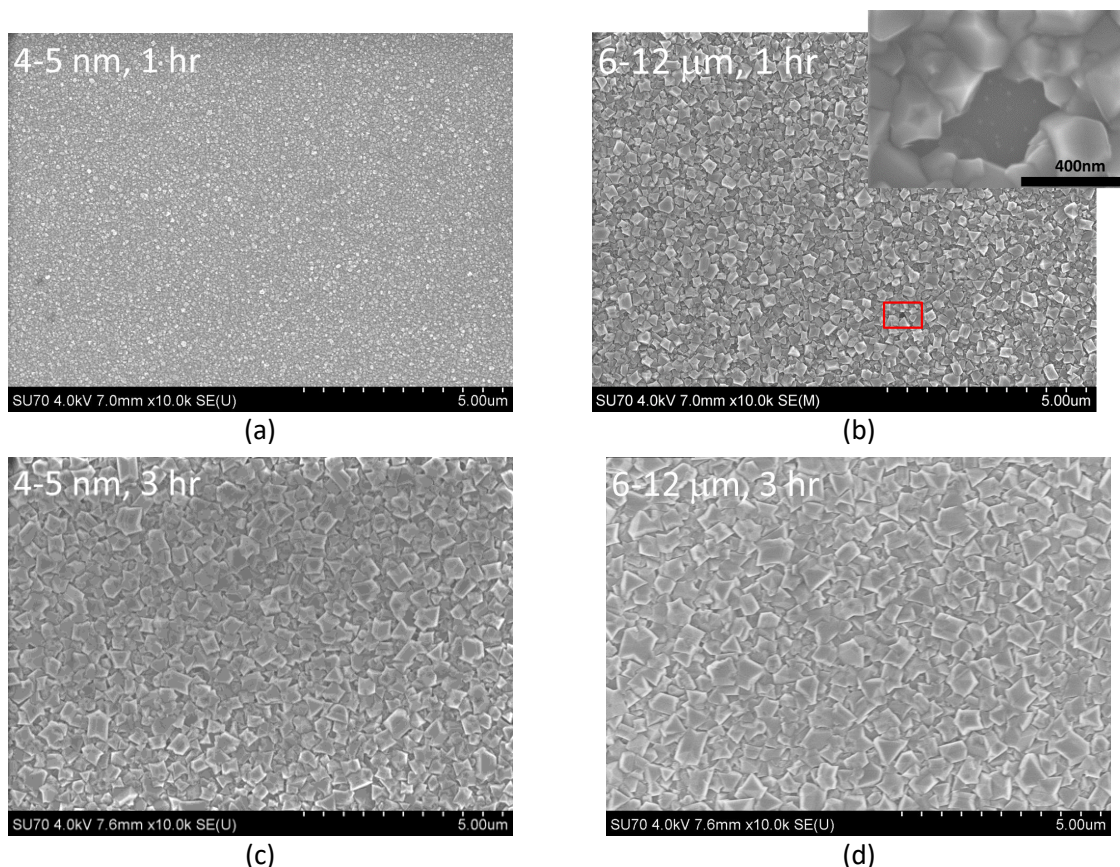

Figure 5. SEM images of samples (a) POL_PT2_S3_G3 and (b) EPI_PT3_S4_G3 (one hour growth); (c) POL_PT2_S3_G4 and (d) EPI_PT3_S4_G4 (three hours growth). (a) inset: magnified view of a hole in film on sample POL_PT2_S3_G3.

Figures 6a and b show the Raman spectra of the diamond films after one and three hours deposition, respectively, for the series C samples. The SiC spectrum is again included as a reference. Raman spectra were obtained from 5 different locations for each sample and they are quite similar, attesting the uniformity of the diamond deposits. After 1 hour of deposition, and despite being closed, the film deposited after DND seeding (POL_PT2_S3_G3) shows a very poor diamond signal, a broad peak with amplitude comparable to the one of the G-band, centered around 1590 cm^{-1}. On the contrary, the

sample EPI_PT3_S4_G3, seeded with 6-12 μm grit, shows a diamond peak centered at ≈1333 cm^{-1} and 20 cm^{-1} full with at half maximum (FWHM); a small band at 1135 cm^{-1} is attributed to the presence of nanocrystalline diamond or trans-polyacetylene and the G-band, if present, is not prominent. It should be noted, however, that the Raman spectrum of the SiC substrate has a band at ≈1525 cm^{-1}, which may be partially superimposed on the G band thus hampering its proper identification. After 3 hours growth the diamond peak sharpens for both samples (FWHM of 19 and 16 cm^{-1} for samples seeded with DND and grit, respectively) and the G-band contribution (reflected in the amplitude ratio between the sp^3 peak and the G-band) decreases clearly. Once again, since the superposition of the SiC 1525 cm^{-1} band hampers the accurate determination of the amplitude of the G-band, we opted not to quantify it. The comparison of the Raman spectra of the different samples suggests that, even though the nucleation density obtained with DND particles may be larger than the one obtained with 6-12 μm grit, seeding with grit improves the quality of the initial layers of the diamond deposits in comparison to seeding with these particular DND particles – and this is advantage when the diamond films are intended to passivate surface electric defects or to extract heat from a particular device. This difference in quality can be due to the presence of the amorphous carbon / graphitic shell surrounding the sp^3 cluster. DND powders synthesized by detonation contain core particles with a size of 4-5 nm agglomerated in primary, secondary and larger aggregates. The larger and secondary aggregates can be broken down into primary aggregates with diameters of 100-200 nm by ultrasonic treatments, but the further breaking of these primary aggregates into the 4-5 nm core particles requires a more energetic technique, typically bead milling [5]. However, this approach introduces contamination from the bead material and creates an sp^2 shell on the surface of the DND core particles [42],[7] whose removal requires further processing methods like treatment with super-critical water, ozone, oxidizing acids or boric anhydride [10]. It has been shown that exposure of DND seeds to H$_2$ plasma in a microwave plasma CVD (MPCVD) system at 720°C for 5 and 15 minutes reduces the C-C sp^2 XPS peak down to 10 and <5%, respectively, in comparison with the same peak in the un-hydrogenated seeds [44]. In the present study, samples were deposited in a HFVCD system (with a lower concentration of atomic H) and at considerably lower temperatures. The combined effect of atomic H etching and sp^3 growth due to the presence of CH$_4$ is thus not expected to lead to the total etching of the amorphous shell. These results outline the importance of using DND particles that have been further processed to remove the outer sp^2 shell when the quality of the diamond film at the interface is of utmost importance, as is the case when passivation of electronic devices or improved heat extraction are required.
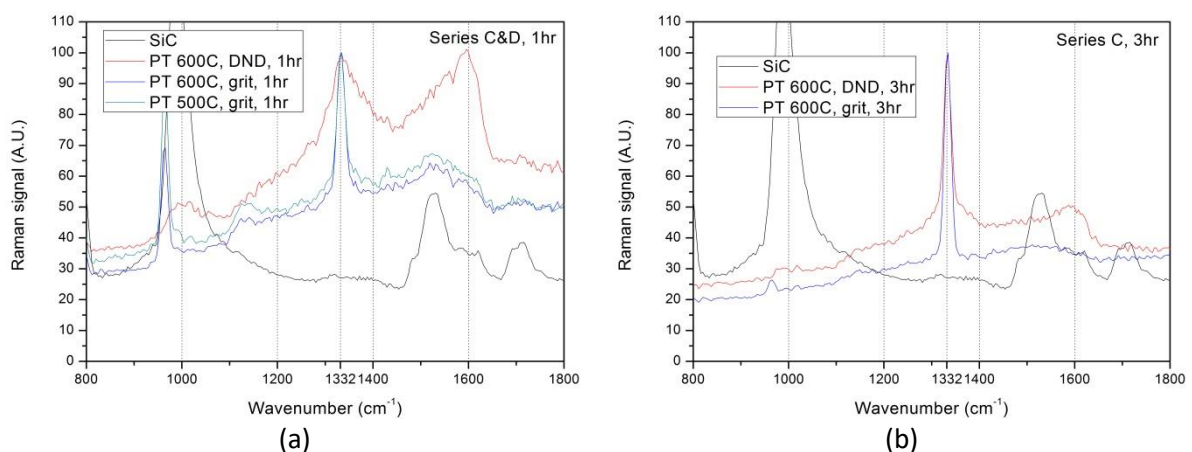

Figure 6. Raman spectra of samples (a) POL_PT2_S3_G3, EPI_PT3_S4_G3 and EPI_PT4_S5_G5 (one hour growth); (b) POL_PT2_S3_G4 and EPI_PT3_S4_G4 (three hours growth). SiC spectrum shown as a reference.

Finally, in order to depict the influence (if any) of the PT temperature, an epitaxial SiC substrate was given PT for one hour at 500 °C. Seeding was performed with 6-12 μm diamond grit and diamond was deposited at 500 °C for one hour (sample EPI_PT4_S5_G5). SEM images (Figure 7) reveal the diamond film is not closed and the crystal size is comprised between 125-225 nm, whereas the crystal size of the sample prepared under similar conditions but with PT performed at 600°C (EPI_PT3_S4_G3) was somewhat larger (150-350 μm). It is known that the carbon atoms in the PT film act as an additional carbon supply during the initial stages of diamond growth, promoting lateral growth and the film coalescence [33]. On the other hand, the PT film thickness increases with temperature, meaning that for a lower deposition temperature the amount of C incorporated in the PT film is lower. As a consequence, and even though the deposition conditions were similar for both EPI_PT3_S4_G3 and EPI_PT4_S5_G5, the total supply of C atoms in the case of sample EPI_PT4_S5_G5 was smaller and the film did not coalesce fully in one hour. The Raman spectrum of sample EPI_PT4_S5_G5 (Figure 6a) is similar to the Raman spectrum of sample EPI_PT3_S4_G3 .This suggests that the conditions of a particular PT cycle play a vital role in the incubation time of the diamond film (as the carbon content of the PT film increases the grains coalesce faster, thus decreasing coalescence time) but do not influence the quality (almost identical FWHM values in Table 16) of the final deposits.
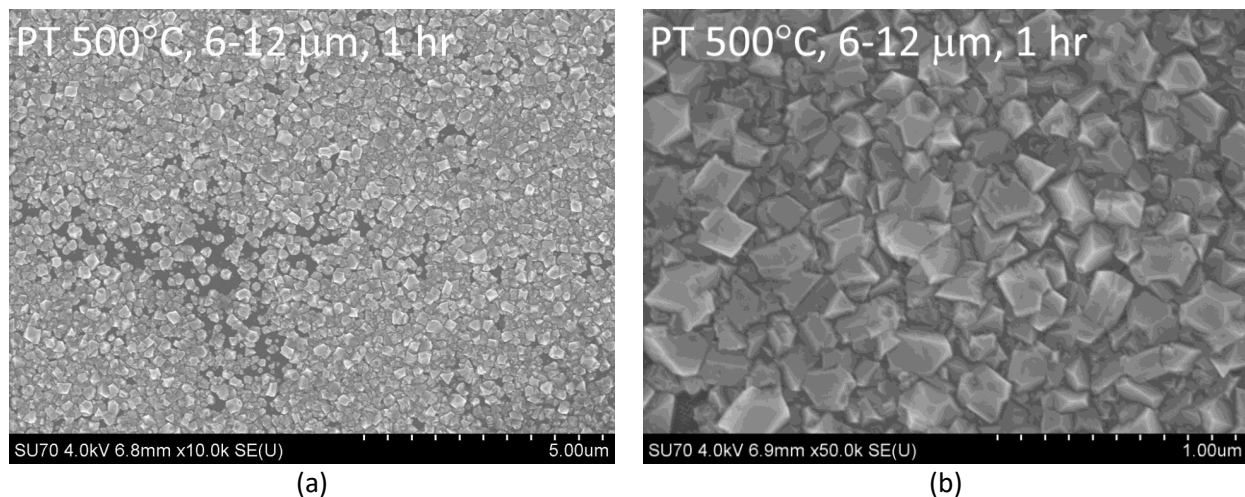

Figure 7. (a, b) SEM images of sample EPI_PT4_S5_G5.

4. Conclusions

Thin diamond films were deposited on SiC substrates using HFCVD at temperatures as low as 500 °C; seeding was performed with 4-5 nm DND, 6-12 and 50-60 μm diamond suspensions. Some of the substrates were partially covered during the PT step with a Si piece; SEM images suggest that this piece induced the trapping of activated species immediately below the edges of the Si piece, which in turn cause the deposited films to be highly non-homogeneous. Lower deposition temperatures (500 °C) induce the lateral growth of the diamond crystals, in comparison to higher temperatures (600 °C). Seeding with 40-60 μm grit was not effective, since the SiC substrates only showed isolated crystals. On the contrary, after 1 hour CVD at 500 °C the sample seeded with DND showed a completely closed diamond film but isolated small holes could be seen in the sample seeded with 6-12 μm. However, the quality of the film obtained with 6-12 μm seeding was considerable better than the quality of the one obtained with DND seeding (FWHM of 16 and 19 cm^{-1} after 3 hours deposition, respectively), suggesting that the DND seeds used in this study had an outer sp^2 shell. The temperature at which the PT film was

formed was shown to have an impact on the incubation time of the diamond deposits: an increase in the PT temperature leads to a larger incorporation of carbon atoms in the PT film and a consequent decrease in the incubation time.

5. Acknowledgements

6. References

[1]   R. Eden, SiC and GaN Electronics: Where, When, and How Big?, Compd. Semicond. (2012) 1–4. http://www.compoundsemiconductor.net/article/89752-sic-and-gan-electronics-where,-when-and-how-big.html.

[2]   C.M. Zetterling, A. Hallén, R. Hedayati, S. Kargarrazi, L. Lanni, B.G. Malm, S. Mardani, H. Norström, A. Rusu, S.S. Suvanam, Y. Tian, M. Ostling, Bipolar integrated circuits in SiC for extreme environment operation, Semicond. Sci. Technol. 32 (2017) 034002. doi:10.1088/1361-6641/aa59a7.

[3]   S. Iijima, Y. Aikawa, K. Baba, Early formation of chemical vapor deposition diamond films, Appl. Phys. Lett. 57 (1990) 2646–2648. doi:10.1063/1.103812.

[4]   Y. Mitsuda, Y. Kojima, T. Yoshida, K. Akashi, The growth of diamond in microwave plasma under low pressure, J. Mater. Sci. 22 (1987) 1557–1562. doi:10.1007/BF01132374.

[5]   O.A. Williams, O. Douhéret, M. Daenen, K. Haenen, E. Osawa, M. Takahashi, Enhanced diamond nucleation on monodispersed nanocrystalline diamond, Chem. Phys. Lett. 445 (2007) 255–258. doi:10.1016/j.cplett.2007.07.091.

[6]   A. Kromka, Š. Potocký, J. Čermák, B. Rezek, J. Potměšil, J. Zemek, M. Vaněček, Early stage of diamond growth at low temperature, Diam. Relat. Mater. 17 (2008) 1252–1255. doi:10.1016/j.diamond.2008.03.035.

[7]   O. Shenderova, S. Hens, G. McGuire, Seeding slurries based on detonation nanodiamond in DMSO, Diam. Relat. Mater. 19 (2010) 260–267. doi:10.1016/j.diamond.2009.10.008.

[8]   J.E. Butler, A. V. Sumant, The CVD of nanodiamond materials, Chem. Vap. Depos. 14 (2008) 145–160. doi:10.1002/cvde.200700037.

[9]   A.K. Mallik, J.C. Mendes, S.Z. Rotter, S. Bysakh, Detonation Nanodiamond Seeding Technique for Nucleation Enhancement of CVD Diamond – Some Experimental Insights, Adv. Ceram. Sci. Eng. 3 (2014) 36–45. doi:10.14355/acse.2014.03.005.

[10]   A. Krueger, D. Lang, Functionality is key: Recent progress in the surface modification of nanodiamond, Adv. Funct. Mater. 22 (2012) 890–906. doi:10.1002/adfm.201102670.

[11]   S. Mandal, E.L.H. Thomas, C. Middleton, L. Gines, J.T. Griffiths, M.J. Kappers, R.A. Oliver, D.J. Wallis, L.E. Goff, S.A. Lynch, M. Kuball, O.A. Williams, Surface Zeta Potential and Diamond Seeding on Gallium Nitride Films, ACS Omega. 2 (2017) 7275–7280. doi:10.1021/acsomega.7b01069.

[12]   S.S. Nicley, S. Drijkoningen, P. Pobedinskas, J. Raymakers, W. Maes, K. Haenen, Growth of Boron-

Doped Diamond Films on Gold-Coated Substrates with and without Gold Nanoparticle Formation, Cryst. Growth Des. 19 (2019) 3567–3575. doi:10.1021/acs.cgd.9b00488.

[13] S. Yugo, T. Kanai, T. Kimura, T. Muto, S. Yugo, T. Kanai, T. Kimura, T. Muto, Generation of diamond nuclei by electric field in plasma chemical vapor deposition Generation deposition of diamond nuclei by electric field in plasma chemical vapor, 1036 (2001) 1036–1038. doi:10.1063/1.104415.

[14] B.R. Stoner, G.H.M. Ma, S.D. Wolter, J.T. Glass, Characterization of bias-enhanced nucleation of diamond on silicon by invacuo surface analysis and transmission electron microscopy, Phys. Rev. B. 45 (1992) 11067–11084. doi:10.1103/PhysRevB.45.11067.

[15] M. Mayr, C. Stehl, M. Fischer, S. Gsell, M. Schreck, Correlation between surface morphology and defect structure of heteroepitaxial diamond grown on off-axis substrates, Phys. Status Solidi Appl. Mater. Sci. 211 (2014) 2257–2263. doi:10.1002/pssa.201431210.

[16] K.H. Lee, S. Saada, J.C. Arnault, R. Moalla, G. Saint-Girons, R. Bachelet, H. Bensalah, I. Stenger, J. Barjon, A. Tallaire, J. Achard, Epitaxy of iridium on SrTiO 3 /Si (001): A promising scalable substrate for diamond heteroepitaxy, Diam. Relat. Mater. 66 (2016) 67–76. doi:10.1016/j.diamond.2016.03.018.

[17] J. Kusterer, P. Schmid, E. Kohn, Mechanical microactuators based on nanocrystalline diamond films, New Diam. Front. Carbon Technol. 16 (2006) 295–321.

[18] M. Kubovic, A. Aleksov, M. Schreck, T. Bauer, B. Stritzker, E. Kohn, Field effect transistor fabricated on hydrogen-terminated diamond grown on SrTiO3 substrate and iridium buffer layer, Diam. Relat. Mater. 12 (2003) 403–407. doi:10.1016/S0925-9635(03)00068-2.

[19] H. Kawashima, H. Noguchi, T. Matsumoto, H. Kato, M. Ogura, T. Makino, S. Shirai, D. Takeuchi, S. Yamasaki, Electronic properties of diamond Schottky barrier diodes fabricated on silicon-based heteroepitaxially grown diamond substrates, Appl. Phys. Express. 8 (2015) 104103 1–4. doi:10.7567/APEX.8.104103.

[20] M.K. Singh, E. Titus, J.C. Madaleno, G. Cabral, J. Gracio, Novel two-step method for synthesis of high-density nanocrystalline diamond fibers, Chem. Mater. 20 (2008) 1725–1732. doi:10.1021/cm0714741.

[21] R. Bogdanowicz, M. Sobaszek, J. Ryl, M. Gnyba, M. Ficek, Ł. Gołuński, W.J. Bock, M.̄mietana, K. Darowicki, Improved surface coverage of an optical fibre with nanocrystalline diamond by the application of dip-coating seeding, Diam. Relat. Mater. 55 (2015) 52–63. doi:10.1016/j.diamond.2015.03.007.

[22] N.A. Fox, M.J. Youh, J.W. Steeds, W.N. Wang, Patterned diamond particle films, J. Appl. Phys. 87 (2000) 8187–8191. doi:10.1063/1.373516.

[23] Y.C. Chen, Y. Tzeng, A.J. Cheng, R. Dean, M. Park, B.M. Wilamowski, Inkjet printing of nanodiamond suspensions in ethylene glycol for CVD growth of patterned diamond structures and practical applications, Diam. Relat. Mater. 18 (2009) 146–150. doi:10.1016/j.diamond.2008.10.004.

[24] A.F. Sartori, P. Belardinelli, R.J. Dolleman, P.G. Steeneken, M.K. Ghatkesar, J.G. Buijnsters, Inkjet-Printed High-Q Nanocrystalline Diamond Resonators, Small. 15 (2019) 1803774 1–11. doi:10.1002/smll.201803774.

[25] J. Hees, A. Kriele, O.A. Williams, Electrostatic self-assembly of diamond nanoparticles, Chem. Phys. Lett. 509 (2011) 12–15. doi:10.1016/j.cplett.2011.04.083.

[26] T. Yoshikawa, F. Gao, V. Zuerbig, C. Giese, C.E. Nebel, O. Ambacher, V. Lebedev, Pinhole-free ultra-thin nanocrystalline diamond film growth via electrostatic self-assembly seeding with increased salt concentration of nanodiamond colloids, Diam. Relat. Mater. 63 (2016) 103–107. doi:10.1016/j.diamond.2015.08.010.

[27] J.G. Buijnsters, L. Vázquez, J.J. ter Meulen, Substrate pre-treatment by ultrasonication with diamond powder mixtures for nucleation enhancement in diamond film growth, Diam. Relat.

Mater. 18 (2009) 1239–1246. doi:10.1016/j.diamond.2009.04.007.

[28]   H. Buchkremer-Hermanns, H. Ren, H. Weiβ, Optimization of diamond nucleation and growth using MW-PACVD method, Diam. Relat. Mater. 5 (1996) 312–316. doi:10.1016/0925-9635(95)00353-3.

[29]   L. Demuynck, J.C. Arnault, C. Speisser, R. Polini, F. Le Normand, Mechanisms of CVD diamond nucleation and growth on mechanically scratched and virgin Si(100) surfaces, Diam. Relat. Mater. 6 (1997) 235–239. doi:10.1016/s0925-9635(96)00709-1.

[30]   J.C. Mendes, H.L. Gomes, S.C. Trippe, D. Mukherjee, L. Pereira, Small signal analysis of MPCVD diamond Schottky diodes, Diam. Relat. Mater. 93 (2019) 131–138. doi:10.1016/j.diamond.2019.02.008.

[31]   W.L. Liu, M. Shamsa, I. Calizo, A.A. Balandin, V. Ralchenko, A. Popovich, A. Saveliev, Thermal conduction in nanocrystalline diamond films: Effects of the grain boundary scattering and nitrogen doping, Appl. Phys. Lett. 89 (2006) 17–19. doi:10.1063/1.2364130.

[32]   J. Anaya, T. Bai, Y. Wang, C. Li, M. Goorsky, T.L. Bougher, L. Yates, Z. Cheng, S. Graham, K.D. Hobart, T.I. Feygelson, M.J. Tadjer, T.J. Anderson, B.B. Pate, M. Kuball, Simultaneous determination of the lattice thermal conductivity and grain/grain thermal resistance in polycrystalline diamond, Acta Mater. 139 (2017) 215–225. doi:10.1016/j.actamat.2017.08.007.

[33]   S.Z. Rotter, J.C. Madaleno, Diamond CVD by a combined plasma pretreatment and seeding procedure, Chem. Vap. Depos. 15 (2009) 209–216. doi:10.1002/cvde.200806745.

[34]   D. Mukherjee, R. Polini, V. Valentini, S.Z. Rotter, J.C. Mendes, HFCVD nanostructured diamond films deposited by a combination of seeding suspensions and novel nucleation process, Int. J. Surf. Sci. Eng. 11 (2017) 225–240. doi:10.1504/ijsurfse.2017.085622.

[35]   A. V. Sumant, P.U.P.A. Gilbert, D.S. Grierson, A.R. Konicek, M. Abrecht, J.E. Butler, T. Feygelson, S.S. Rotter, R.W. Carpick, Surface composition, bonding, and morphology in the nucleation and growth of ultra-thin, high quality nanocrystalline diamond films, Diam. Relat. Mater. 16 (2007) 718–724. doi:10.1016/j.diamond.2006.12.011.

[36]   W.L. Liu, M. Shamsa, I. Calizo, A.A. Balandin, V. Ralchenko, A. Popovich, A. Saveliev, Thermal conduction in nanocrystalline diamond films: Effects of the grain boundary scattering and nitrogen doping, Appl. Phys. Lett. 89 (2006) 89–91. doi:10.1063/1.2364130.

[37]   Diamond Materials, The CVD diamond booklet, (2014). http://www.diamond-materials.com/downloads/cvd_diamond_booklet.pdf.

[38]   H. Watanabe, N. Yamada, M. Okaji, Linear thermal expansion coefficient of silicon from 293 to 1000 K, Int. J. Thermophys. 25 (2004) 221–236. doi:10.1023/B:IJOT.0000022336.83719.43.

[39]   M. Stockmeier, R. Müller, S.A. Sakwe, P.J. Wellmann, A. Magerl, On the lattice parameters of silicon carbide, J. Appl. Phys. 105 (2009) 033511–4. doi:10.1063/1.3074301.

[40]   E. Salgueiredo, M. Amaral, M.A. Neto, A.J.S. Fernandes, F.J. Oliveira, R.F. Silva, HFCVD diamond deposition parameters optimized by a Taguchi Matrix, Vacuum. 85 (2011) 701–704. doi:10.1016/j.vacuum.2010.10.010.

[41]   V.N. Mochalin, O. Shenderova, D. Ho, Y. Gogotsi, The properties and applications of nanodiamonds, Nat. Nanotechnol. 7 (2012) 11–23. doi:10.1038/nnano.2011.209.

[42]   E. Ōsawa, Monodisperse single nanodiamond particulates, Pure Appl. Chem. 80 (2008) 1365–1379. doi:10.1351/pac200880071365.

[43]   Y. Liang, M. Ozawa, A. Krueger, A general procedure to functionalize agglomerating nanoparticles demonstrated on nanodiamond, ACS Nano. 3 (2009) 2288–2296. doi:10.1021/nn900339s.

[44]   J.C. Arnault, S. Saada, M. Nesladek, O.A. Williams, K. Haenen, P. Bergonzo, E. Osawa, Diamond nanoseeding on silicon: Stability under H2 MPCVD exposures and early stages of growth, Diam. Relat. Mater. 17 (2008) 1143–1149. doi:10.1016/j.diamond.2008.01.008.